Building Engineering 2024, 2(1), 470.
https://doi.org/10.59400/be.v2i1.470

Article

Comprehensive seismic loss model of Tehran, Iran in the case of Mosha fault seismic scenario using stochastic finite-fault method

Nazila Kheirkhah[1], Reza Alikhanzadeh[2], Ozhan Musavi[2], Ali Aghajani[2], Erfan Firuzi[2,*]

[1] Institute of Geophysics, University of Tehran, Tehran 1435944411, Iran
[2] International Institute of Earthquake Engineering and Seismology (IIEES), Tehran 1953714453, Iran
*** Corresponding author:** Erfan Firuzi, e.firuzi@iiees.ac.ir

CITATION

Kheirkhah N, Alikhanzadeh R, Musavi O, et al. Comprehensive seismic loss model of Tehran, Iran in the case of Mosha fault seismic scenario using stochastic finite-fault method. Building Engineering. 2024; 2(1): 470. https://doi.org/10.59400/be.v2i1.470

ARTICLE INFO

Received: 9 January 2024
Accepted: 29 January 2024
Available online: 2 April 2024

Abstract: This paper presents the results of a study caried out to assess probable seismic loss, in term of damage to the residential buildings and the number of fatalities, in the case of Mosha Fault seismic scenario in Tehran, Iran. Accordingly, seismic risk components (including seismic hazard, exposure model and fragility curves) are evaluated. The stochastic finite-fault method with dynamic corner frequency is applied for quantifying ground motion values. The results shows that PGA on the soil surface could range between 0.1 g to 0.45 g. Then, a reliable model of building exposure by analyzing census data from Tehran is compiled. This model included 19 different classes of buildings and is used to evaluate the potential damage to buildings from seismic scenario. The results indicate that the median of damage ratio from 100,000 iterations for the whole of the city is about 6% ± 1.54%. The study found that the central and eastern parts of Tehran are the most vulnerable areas, with an estimated 15,952 residents at risk of losing their lives in this scenario. This is equivalent to 0.2 percent of total population of Tehran. The finding from this study can be used by local authorities to provide appropriate emergency-response and preparedness plans in the case of Mosha Fault seismic scenario.

Keywords: stochastic finite-fault model; seismic risk; building damages; casualty; Tehran

1. Introduction

The Iranian plateau is a wide zone of compressional deformation along the active Alpine-Himalayan seismic belt, resulting from the convergence of the Eurasian and Arabian plates [1,2]. This region is considered one of the most seismically prone regions in the world. Buin-Zahra (7.1 Mw, 1962), Tabas (7.4 Mw, 1978), Manjil-Roudbar (7.4 Mw, 1990), Bam (6.6 Mw, 2003), and Sarpole-Zahab (7.3 Mw, 2017) are among the most catastrophic seismic events that have occurred in Iran during the last few decades. According to the global catalog of UTSU, more than 92,000 individuals lost their lives in these earthquakes. This demonstrates the country's high seismic risk and highlights the importance of implementing appropriate seismic risk reduction plans in major cities of the country.

Tehran, the capital of Iran, as the most populated city in Iran, is also exposed to high seismic risk. Based on the latest data from the Statistical Center of Iran (SCI), the population of the city was around 8,737,510 in 2016. Tehran also contributes more than 30% to the gross domestic product of the country [3]. In addition, the majority of economic, social, and political centers are located in Tehran. Consequently, its safety and security against natural and man-made hazards are crucial for the government.

Tectonically, Tehran is located on the southern edge of the central Alborz Mountain belt. This region is characterized by discontinuities, with many active faults

in or around the city [4]. The major active faults in or around Tehran are Mosha, North Tehran Fault (NTF), Ray and Taleghan (**Figure 1**). These are the sources of several devastating historical earthquakes, as listed in **Table 1**. Mosha fault, with an approximate length of 220 km, is the causative fault for most of the historical earthquakes in this region. By considering the time intervals of historical earthquakes that occurred along the Mosha fault, it can be inferred that the return period of major earthquakes is approximately 165 years. The last devastating earthquake in the Tehran region caused by Mosha fault occurred in 1830; thus, more than 190 years have passed since that event. Accordingly, the possibility of a similar strong earthquake occurring in the near future is quite high [5,6]. Such a strong earthquake is likely to cause numerous casualties and severe damage to buildings and infrastructures in Tehran. These issues have also been addressed in the studies of Berberian et al. [7], Firuzi et al. [8], Kalantari et al. [9] and Firuzi et al. [10].

The above explanations show the importance of conducting detailed seismic hazard and risk assessments to address the impact of the Mosha fault scenario on the region. Such studies can play a fundamental role in developing appropriate risk reduction and emergency response plans to deal with the consequences of a potential earthquake.

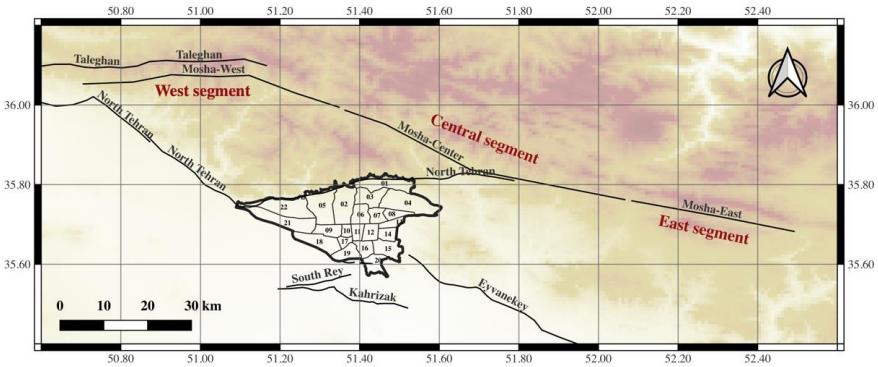

Figure 1. The location of Tehran with respect to the major active faults.

Table 1. List of devastating historical events occurred around Tehran.

Date	Ms	Longitude	Latitude	Causative fault	Reference
855/5/22	7.1	51.5	35.6	Kahrizak	[11]
958/2//23	7.7	51.1	36.0	Taleghan/Mosha	[12]
1177/5/-	7.2	50.7	35.7	North Tehran Fault	[13]
1665/6/15	6.5	52.1	35.7	Mosha	[14]
1815/6/-	7.1	52.2	35.9	Mosha	[14]
1830/3/27	7.1	52.5	35.7	Mosha	[15]

In order to assess seismic risk, the seismic hazard must first be characterized. Then, an exposure model needs to be developed, and appropriate fragility/vulnerability curves should be employed. For seismic hazard assessment, most studies use Ground Motion Prediction Equations (GMPEs), which generally do not address parameters such as directivity or pulse waves. To the authors' knowledge, no work in the literature assesses the seismic loss of Tehran for the Mosha fault seismic

scenario using the finite-fault method. However, this is an appropriate approach for modeling the source, path, and near-surface effects properly. The finite-fault method is especially applicable in regions like Tehran, where the last destructive earthquake dates back to the pre-instrumental period, and there is a lack of recorded strong ground motions from earthquakes on the faults to develop empirical GMPEs. Some of the most recent seismic risk studies in Tehran are introduced as follows.

JICA [16] assessed the seismic risk of Tehran in terms of the number of casualties and economic losses by considering three seismic scenarios, including the rupture of Ray, Mosha, and North-Tehran faults. In that study, GMPEs were used to provide the ground motion shaking map. Their findings showed that the most and least destructive seismic scenarios are the Ray and Mosha faults events, respectively. Based on this study, the rupture of Mosha fault may cause a damage ratio equal to 13% of total buildings with 20,000 deaths, which is equivalent to 0.3% of the total population. By using the stochastic approach proposed by Beresnev [17], Zafarani et al. [18] assessed the seismic hazard of Tehran based on the seismic scenarios of Ray, North Tehran, and Mosha faults. That study showed that the rupture of Mosha fault will generate the highest PGAs, between 0.1 to 0.3 g. However, Zafarani et al. [18] did not perform the seismic risk analysis to identify the most destructive seismic scenarios. Saffari et al. [19] also evaluated the potential seismic hazard of Tehran by considering the rupture of Mosha fault, using the stochastic finite-fault model. They performed their analysis using the EXSIM program. Their results depict that the PGA in Tehran may vary from 0.13 g to 0.55 g in the Mosha fault seismic scenario.

As discussed above, there is no comprehensive study in the literature that has employed the stochastic method for conducting a full seismic risk assessment in Tehran for Mosha seismic scenario. Therefore, this study attempts to estimate seismic loss (in terms of the number of fatalities and damage to residential buildings) using the stochastic finite-fault method for the Mosha fault seismic scenario, which is widely regarded as the most likely seismic scenario in Tehran. In following, first, a description of the stochastic finite-fault approach is presented. Then, the seismic hazard map of Tehran, developed based on the stochastic finite-fault method, is introduced, and the results are compared with GMPEs. Next, the exposure model is described, and employed fragility and vulnerability curves are introduced. Finally, an estimation of the possible losses in terms of building damages and fatalities is presented and discussed.

2. Stochastic finite-fault method

Estimating potential ground motion values of earthquakes in terms of engineering parameters (such as PGA, PGV, Seismic Intensity, or spectral acceleration) is a key step for seismic risk assessment. In practice, the common approach for seismic hazard analysis is GMPE; however, it has some deficiencies, including its dependence on the availability of data on ground motions. In fact, these equations are developed based on the regression of observed ground motions in past earthquakes. Clearly, the lack of sufficient data at different distance or magnitude ranges will affect their accuracy [20]. This is the case in many cities in Iran, such as Tehran, where an adequate number of records (particularly near-source data) is not available. In addition, there are

uncertainties in selecting appropriate functional forms of GMPEs. Moreover, GMPEs only provide strong ground motion parameters rather than time history waveform required for dynamic analysis of important structures. To address these issues, using simulating tools attracts the attention of seismologists and earthquake engineers.

Several simulating methodologies have been proposed in the literature, which vary from simple approaches that replicate certain characteristics of ground motion records to sophisticated physic-based methods that mathematically model the earthquake phenomenon [21]. In the present study, an improved stochastic finite-fault approach developed by Motazedian [22] is employed. An open-source FORTRAN program named EXSIM with high calculation capabilities is also used. EXSIM is an extended version of stochastic point source simulation (stochastic method simulation, SMSIM), developed by Boore [23,24], and finite-fault simulation (FINSIM) approach introduced by Beresnev [17]. The basic premise of EXSIM is dividing the rupture plane into an array of sub-faults treated as point sources, like FINSIM, by introducing the dynamic corner frequency. These improvements overcome two main shortcomings of the aforementioned approaches. The idea of dividing the rupture area into sub-faults provides the capability of EXSIM to simulate large earthquakes and eliminates the limitation to small or moderate magnitude events as SMSIM. In addition, introducing the dynamic corner-frequency eliminates the dependence of the results on the sub-fault size as FINSIM. Based on the above explanations, EXSIM, by superimposing the motion from each sub-fault (as given in Equation (1)), provides the ground motion by considering the rupture and propagation delay.

$$a(t) = \sum_{i=1}^{nl} \sum_{j=1}^{nw} a_{ij}(t + \Delta_{ij}) \tag{1}$$

In the above equation, nl and nw are the number sub-faults along the strike and dip of fault, respectively. Δ_{ij} is the relative delay time from ijth subfaults to the observed point and $a(t)$ represents the simulated ground motion values of the entire fault. The Fourier amplitude of each sub-fault is estimated using the w^2 shape, where w is angular frequency [25].

$$A_{ij}(f) = CH_{ij}M_{0ij}\frac{(2\pi f)^2}{1+\left(\frac{f}{f_{0ij}}\right)^2}e^{-\pi f_{k_0}}\frac{e^{-\frac{\pi f R_{ij}}{Q(f)\beta}}}{R_{ij}}G(R_{ij}) \tag{2}$$

In the above equation, M_{0ij} (dyn.cm) denotes the seismic moment of sub-fault (by considering identical sub-fault, this is equal to $M_{0ij} = M_0/N$), f_{0ij} depicts the dynamic corner frequency of sub-fault, H_{ij} is a scaling factor to be applied to conserve the high frequency spectral level of sub-fault, term $e^{-\pi f_{k_0}}$ is a high cut filter that take into account the near surface attenuation effect, where k_0 is the fast spectral decay at high frequency, $Q(f)$ (with general form of $Q(f) = Q_0 f^n$) is a quality factor represents anelastic and scattering attenuation, ρ (kg/m^3) is density, β (Km/s) is the shear-wave velocity in vicinity of source, R_{ij} (Km) is distance of the sub-fault from the observed point, $G(R_{ij})$ denotes the geometric spreading function, and C is a constant which defined as:

$$C = \frac{R_{\theta\phi} V F}{(4\pi\rho\beta^3 R_0)} \tag{3}$$

where $R_{\theta\phi\sim}0.55$ is radiation pattern (typically 0.55 for shear waves), $F = 2$ is the free surface amplification, $V = 1/\sqrt{2}$ is the partition of total shear-wave energy into two horizontal components, and $R_0 = 1$ km is the reference distance.

As mentioned, EXSIM uses dynamic frequency (f_{0ij}) as given in Equation (4) to remove the dependence of results to sub-fault size [22].

$$f_{oij} = N_R(t)^{-1/3} 4.9E + 6\beta(\frac{\Delta\sigma}{M_{0ave}})^{1/3} \tag{4}$$

In the above equation, $\Delta\sigma$ is stress drop in bar, M_{0ave} is the average seismic moment of subfaults ($M_{0ij} = M_0/N$), and $N_R(t)$ is the cumulative number of ruptured sub-fault at time t. According to Equation (4), as rupture area expands, $N_R(t)$ gradually increases; consequently, the corner frequency reaches the minimum value when the entire fault is ruptured. Thus, the radiated energy at high frequency will decrease ($A_{ij}(h)_{f \gg f_{oij}} \propto f_{oij}^2$). To overcome this issue [22] proposed a scaling factor (H_{ij}) as given in Equation (5) to conserve the energy radiated from a sub-fault at high frequency. In this equation, f_0 is the static corner frequency calculated by the seismic moment alongside stress drop for the entire fault $f_0 = f_{oij}(end) = N^{-1/3} 4.9E + 6\beta(\frac{\Delta\sigma}{M_{oave}})^{1/3}$.

$$H_{ij} = \sqrt{\frac{N\sum f^2/[1+\left(\frac{f}{f_0}\right)^2]}{\sum f^2/[1+\left(\frac{f}{f_{0ij}}\right)^2]}} \tag{5}$$

It should be mentioned that the aforementioned explanations and formulation provide the Fourier spectrum (a_{ij}) of sub-fault, to take the stochastic characteristics into account the Fourier spectrum multiplied into a windowed Gaussian white noise signal in frequency domain. In the following section, a detailed application of this procedure for Mosha fault is described.

3. Application of finite-fault model for Mosha fault seismic scenario

Figure 2 shows the location of the Mosha fault with respect to the Tehran metropolitan area. As depicted, this fault has three main segments with slightly different orientations [26]. The western segment is located in the north of Tehran, parallel to the Taleghan fault. The relation between these two faults is not clear [27]. The central segment is a left-lateral strike-slip fault with an approximate length of 80 km, which intersects with the NTF. The eastern segment is located along the Mosha valley. Seismological evidence shows that the central part, which is the closest segment to Tehran, has the highest seismicity. Thus, this part has been considered the worst-case scenario in this study.

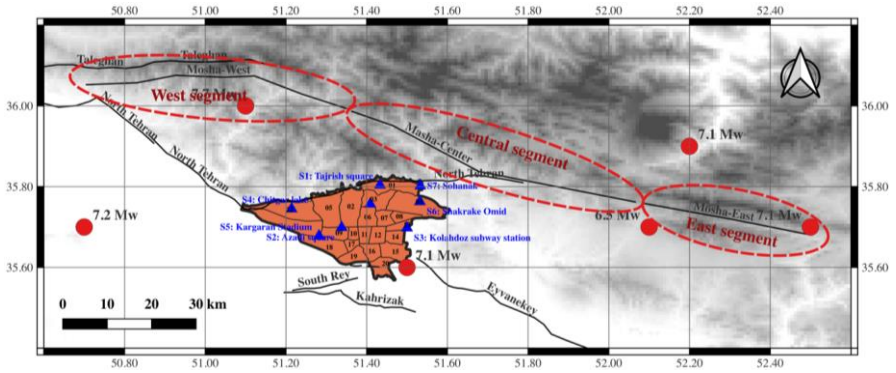

Figure 2. Tectonic map of the Mosha fault in relation to the Tehran Metropolitan; blue triangles are important locations in Tehran which their time history waveforms are depicted as sample (faults are from Solaymani Azad et al. [28]).

In stochastic finite-fault simulation, proper modelling of the plane, dimension of fault, and source parameters are important factors. A summary of the most important model parameters is listed in **Table 2**. According to historical data and the empirical relation of Wells and Coppersmith [29], the potential magnitude of the Mosha fault seismic scenario is estimated to be 7.4 (Mw). This moment magnitude is equivalent to a rupture plane with a length of 75 km and a width of 27 km along the strike and dip of the fault, respectively. The strike and dip of the fault are 283° and 75°, respectively, based on the study by Zafarani et al. [18]. Due to a lack of instrumental strong earthquake records on the Mosha Fault, providing an accurate estimation of stress drop is associated with uncertainties. In this study, a stress drop value of 50 bar is considered, which corresponds to the value proposed by Zafarani et al. [18]. The quality factor in the present study is also taken from the study of Zafarani et al., who proposed the value for earthquakes in the northern part of Iran. This value is extracted from the Manjil-Roudbar earthquake (7.4 Mw, 1990). Similarly, Motazedian [30], based on data from the Manjil-Roudbar earthquake, developed a trilinear geometric spreading function that is used in this study. The percentage of pulsing area is considered to be 50%, which means that during the rupture of sub-faults, at most 50% of all sub-faults could be active while the remaining are passive. This value is proposed by Motazedian [22] based on the concept of self-healing provided by Heaton [31]. It should be noted that due to a lack of information regarding slip distribution, a random normal distribution is considered for analysis.

Based on the aforementioned parameters, the time history waveform is simulated within a square grid cell with a 1 × 1 km dimension for the entire city of Tehran. The distribution of PGA on engineering bedrock within the 22 municipal districts of Tehran is shown in **Figure 3**. As depicted, the PGA values vary between 0.05 to 0.40 g, with maximum values in the northeast of Tehran, which has the closest distance to the Mosha fault. The result has good agreement with the study of Zafarani et al. [18], which used the stochastic approach proposed by Beresnev [17]. It should be noted that for seismic risk assessment, ground motion values on the soil surface are required. For this purpose, the amplification factor provided in the study by JICA [16] is used. In that study, based on information from 450 boreholes, the amplification factor for the entire city of Tehran is derived. **Figure 3** also shows the distribution of PGA on the

soil surface. As shown, by employing the amplification factor, the ground motion values increase, especially in the southern regions of Tehran.

Table 2. Summary of important model parameters for Mosh fault seismic scenario.

Parameter	Value	Reference
Strike, Dip	283°, 75°	[18]
Magnitude	7.4 (Mw)	[18]
Fault dimension along strike and dip	75, 27 (Km)	[29]
Stress drop ($\Delta\sigma$)	50 (bar)	[18]
Sub-fault size	2 × 2 (Km)	-
Shear wave velocity (β)	3.5 (Km/s)	[18]
Density (ρ)	2.8 (kg/m^3)	[18]
Kappa	0.05	[18]
Quality factor	$Q(f) = 87f^{1.47}$	[18]
Geometric spreading	R^{-1} $(R \leq 70)$ $R^{0.2}$ $(75 \leq R \leq 150)$ $R^{-0.1}$ $(R > 150)$	[30]
Pulsing area percentage	50%	[30]
Rupture Velocity	0.8 Shear wave velocity	[30]
Window function	Saragoni-Hart	-
Path duration	0.1R	-

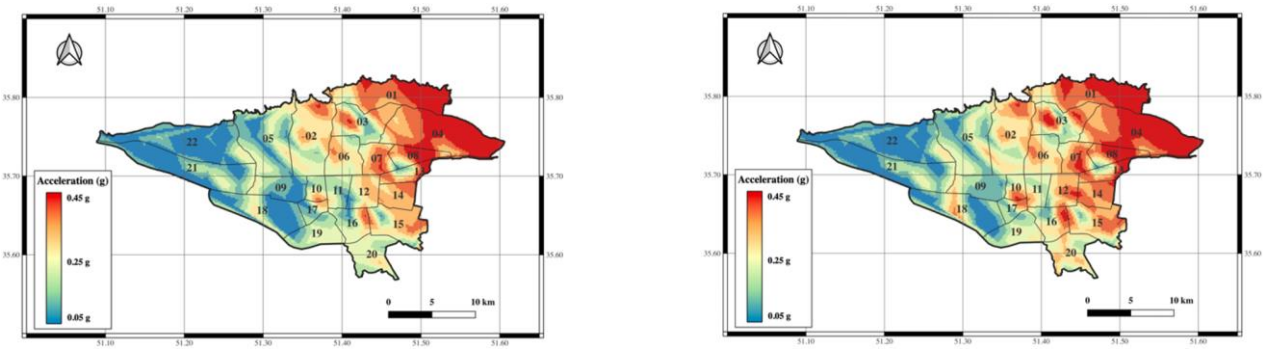

(a) **(b)**

Figure 3. Distribution of PGA within a grid cell of 1 × 1 km in Tehran based on assumed model parameters of Mosha fault seismic scenario. **(a)** on engineering bedrock; **(b)** on soil surface.

Since no strong earthquake has been instrumentally recorded on the Mosha fault, we compared our results with GMPEs. **Figure 4** shows the distribution of PGA derived from the stochastic finite-fault model and the NGA-west2 relations. The circles represent simulation results, while the black thick-dash line represents the fitted curve to simulated data. As depicted, there is appropriate consistency between the values of the stochastic finite-fault model and GMPEs, especially at short distances. It should be noted that there is some inter-event variability in the simulated data that should be considered in the analysis. This is discussed in detail in section 5.

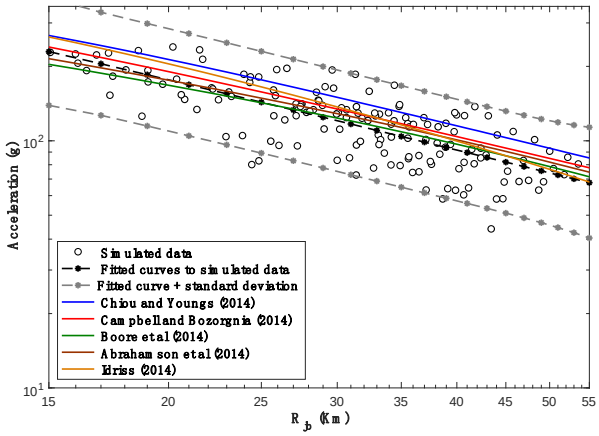

Figure 4. Comparison the PGA values derived from stochastic finite fault model (black circle) and NGA-west2 relations (black thick line is the mean of all GMPEs).

In **Figure 5**, the simulated time history waveform for the eight important locations in Tehran (represented by blue triangles in **Figure 2**) is presented. As shown, the time history waveform of points in the east of Tehran has a short duration with greater amplitude, while the time history waveform of points in the west of Tehran (which are far from the Mosha fault) has a longer duration with weaker amplitude. This is in accordance with our expectations. The pseudo response acceleration for the same locations is also provided in **Figure 6**.

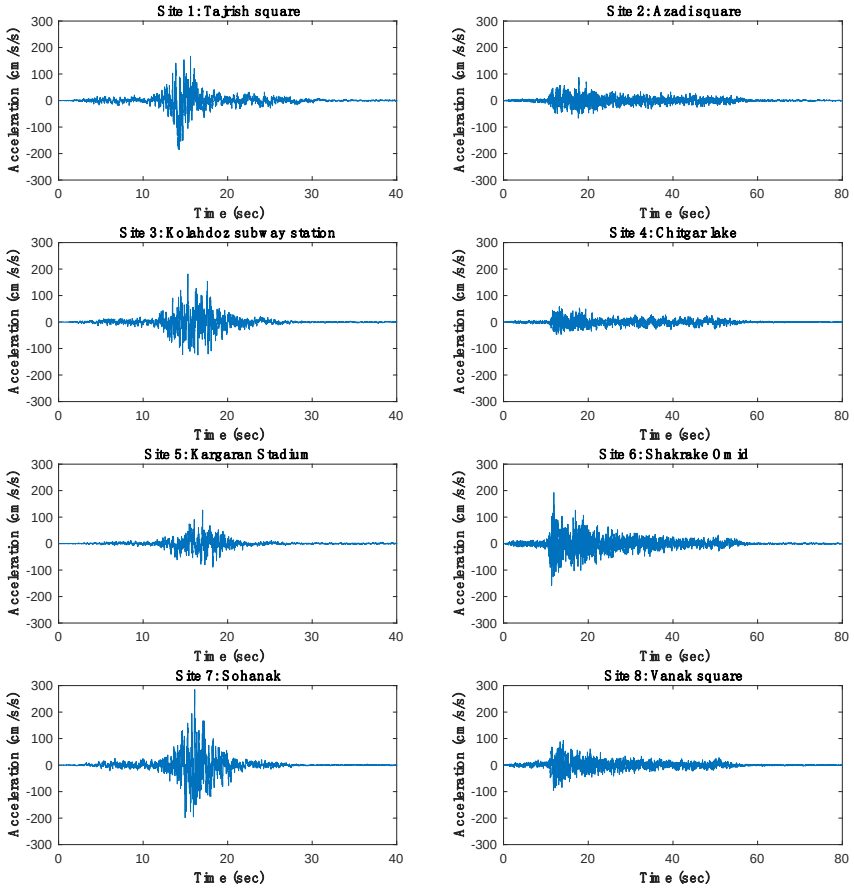

Figure 5. The time history waveform of 8 selected sites in Tehran.

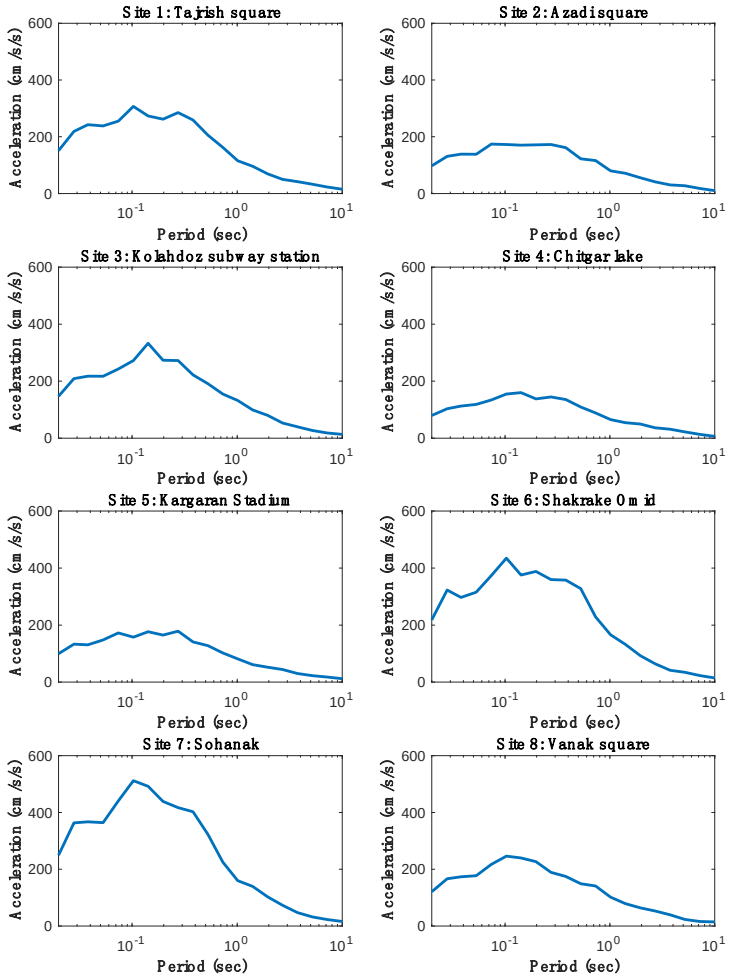

Figure 6. Pseudo response acceleration of the 8 selected sites in Tehran.

4. Compiling exposure model and selecting appropriate fragility curves

To assess the impact of earthquakes, it is necessary to compile a reliable database containing information about the building stock and population distribution in the area. In large-scale seismic risk assessment, buildings are generally categorized into different classes according to their likelihood of sustaining damage at different intensities. In the last few decades, several building taxonomies have been proposed, including ATC-13 [32], the European Macroseismic Scale (EMS-98) [33], HAZUS [34], PAGER-STR [35], Syner-G [36], and GEM [37] taxonomy. A comprehensive review of these classification methods can be found by Crowley et al. [36]. However, the application of these methods in regions like Iran is associated with uncertainties due to a lack of information about building characteristics. For instance, the HAZUS building classification focuses on the structural aspects of a building, while such detailed information about the seismic load resistance of buildings is not available in Iran. Therefore, in seismic loss assessment studies in Iran, most researchers consider a limited number of building taxonomies, considering available data such as construction material, age, and height of buildings. Certainly, considering such generic factors in building classification imposes uncertainties on results. On the other hand,

employing a set of unrealistic assumptions for building classification imposes greater uncertainty on the outcomes.

In the present study, information provided by the Statistical Center of Iran (SCI) is used to compile building taxonomies. SCI is the official authority for data collection on population and buildings in Iran. The latest data from SCI [3] is used, which is the most reliable and available information. SCI provides information on construction material and the age of buildings. Regarding construction material, SCI's information is limited to three groups: Concrete (RC), steel (ST), and masonry (M). In this classification, adobe, masonry, rubble stone, and other types of structures are considered as masonry. By using the year of construction, the quality of buildings or the level of implementation of seismic regulations and codes can be estimated. The Iranian Code of Practice for Seismic Resistant Design of Buildings (Standard No. 2800) is the primary reference for seismic design of structures. To date, four versions of this standard have been developed and published by the Building and Housing Research Center (BHRC). The first edition was released in 1987, and buildings constructed based on this version are considered low-code. The second edition was published in 1996, and buildings designed according to this version are considered mid-code. The third and fourth versions were presented in 2005 and 2015, respectively. Buildings designed based on these versions are considered high-code.

Figure 7 shows the distribution of buildings in Tehran based on the quality and material of construction. As depicted, the majority of buildings are mid-quality steel and low-quality masonry, making them vulnerable to strong earthquakes. To improve the accuracy of building classification, the height of the building was also considered in this study. This factor was extracted from an additional database provided by Tehran Municipality. Based on the number of stories, buildings are classified into three groups: low-rise (less than 4 stories), mid-rise (between 4 to 6 stories), and high-rise (more than 7 stories). By considering the aforementioned factors (i.e., construction material, quality of construction, and height of the building), buildings are classified into 19 classes in this study. The number of different building categories within 22 municipal districts of Tehran is presented in **Table 3**.

Figure 8 shows the spatial distribution of buildings within a grid cell of 1 × 1 km in Tehran. As illustrated, many buildings are located in the eastern and central parts of the city, which are closer to the Mosha fault. Thus, there is a higher seismic risk in these regions in the case of a Mosha fault seismic scenario.

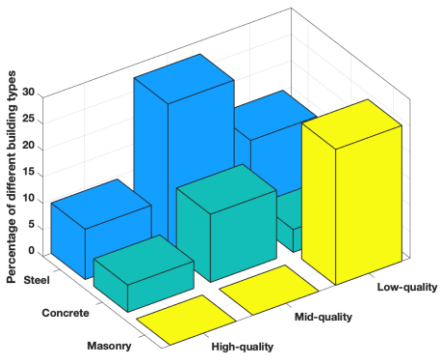

Figure 7. Distribution of buildings in Tehran based on the quality and construction material.

Table 3. Distribution of different building types in 22 municipal districts of Tehran (abbreviations are as follow: ST: steel, RC: concrete, MA: masonry, LR: low-rise, MR: mid-rise, HR: high-rise, LQ: low-quality, MQ: mid-quality, and HQ: high-quality).

District No	ST-LR-LQ	ST-LR-MQ	ST-LR-HQ	ST-MR-LQ	ST-MR-MQ	ST-MR-HQ	ST-HR-LQ	ST-HR-MQ	ST-HR-HQ	RC-LR-LQ	RC-LR-MQ	RC-LR-HQ	RC-MR-LQ	RC-MR-MQ	RC-MR-HQ	RC-HR-LQ	RC-HR-MQ	RC-HR-HQ	MA-LR-LQ	Sum
1	3393	6288	1628	8733	26405	8866	3003	9717	3328	2165	5144	1165	5850	22920	6616	1980	8928	2584	19069	147783
2	5702	9299	2289	14769	38052	11912	3265	9468	2817	3296	10421	1939	7939	40085	12931	2644	13483	3265	18945	212521
3	4323	6280	1271	11061	22820	5574	4072	8221	1959	1730	2736	708	4816	11457	3489	2005	4513	1321	10997	109350
4	10634	22505	6917	27179	77391	25716	2972	10160	3004	2036	5555	1987	5422	20283	9001	960	3779	1262	59311	296074
5	1070	9249	2262	3935	46641	14237	478	6830	2413	4791	16124	5161	9295	74915	30714	3905	11263	4743	7897	255922
6	5611	4113	1026	11928	12073	3346	3711	3251	812	1973	1671	432	4275	5156	1548	1368	1572	449	13254	77570
7	7992	9426	2531	16382	23030	6233	2303	2208	527	1161	1646	510	2542	4545	1596	316	439	260	40050	123695
8	8713	9259	4481	20495	28000	12735	1917	3042	1177	845	1180	528	2198	4009	1831	202	438	167	42860	144078
9	3727	1798	1119	6803	4305	2461	450	180	129	2250	929	758	3829	2157	1671	357	89	80	31113	64206
10	5820	9261	3787	11605	20000	7964	332	418	156	2038	3569	1687	3880	7735	3534	107	157	78	37302	119431
11	4661	8270	2744	11008	21126	7055	840	1165	376	1632	3542	1536	3915	9302	3941	245	454	225	27570	109606
12	4312	5451	2281	9479	15290	6472	927	1476	578	784	1164	796	1712	3016	2025	128	236	131	30101	86359
13	4692	9462	3519	12019	27190	10472	1077	2304	934	393	301	92	925	1126	412	82	99	26	23927	99053
14	12062	15610	6085	24259	39705	14904	2296	2526	834	293	708	175	592	1890	477	75	115	16	52317	174938
15	14821	19716	6180	25744	41606	12840	968	1331	554	1323	957	430	2607	3619	1211	21	385	45	103034	237389
16	7501	6062	2394	12800	12979	4825	670	600	199	1111	1349	359	1926	3455	834	92	39	21	57937	115151
17	5354	2877	2783	9783	6242	5959	508	220	252	2045	1122	1587	3179	2332	3073	176	105	158	49154	96908
18	4162	6850	3401	8754	15821	7973	281	388	187	2607	5277	4092	4997	11774	9039	141	333	238	47812	134127
19	3830	8342	2778	9452	21109	7504	452	878	305	356	805	543	753	1945	1447	77	63	34	16071	76747
20	6247	8144	3012	13865	21939	8706	754	1388	475	1077	2784	958	2293	6701	2545	61	262	65	37691	118966
21	1451	4489	843	2651	12385	2898	675	1394	242	685	2676	811	1145	6665	2640	178	866	183	13269	56149
22	768	2019	197	1434	8675	1590	214	1656	336	335	1397	440	535	7441	5179	158	1518	1320	3841	39053
Sum	126846	184770	63529	274137	542783	190243	32163	68823	21591	34924	71057	26695	74624	252531	105755	15278	49136	16670	743521	2895076

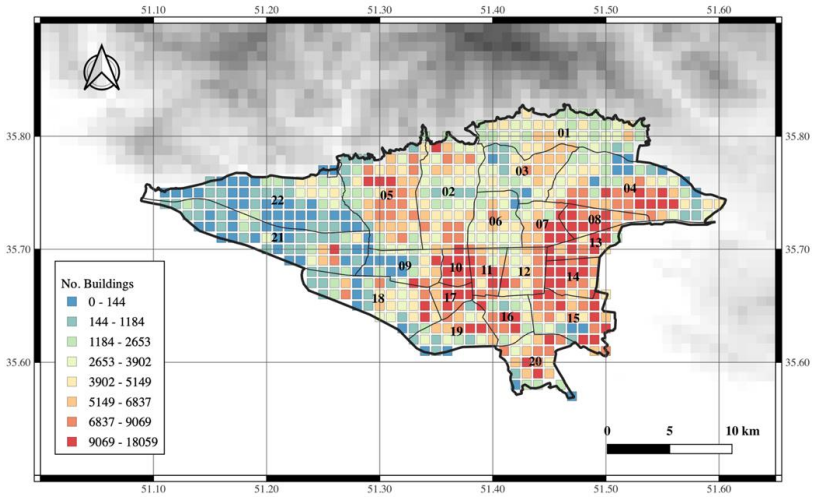

Figure 8. Distribution of buildings in a grid cell of 1 × 1 km within Tehran.

For seismic risk assessment, a set of fragility curves corresponding to the pre-defined building classes is required. Several fragility curves for typical residential buildings in Iran have been proposed by different scholars. In a study performed by the Japan International Cooperation Agency (JICA) [16], nine fragility curves were developed for seismic risk assessment in Tehran. JICA [16] classified the buildings according to their construction material and age. Omidvar et al. [38] developed empirical fragility curves for steel and concrete structures based on data from past earthquakes in Iran, mainly the 1990 Manjil-Roudbar (Mw: 7.4) and 2003 Bam (Mw: 6.6) earthquakes. Sadeghi et al. [39] developed vulnerability curves for 42 building types in Iran by compiling a set of local and global fragility/vulnerability curves and combining them based on engineering judgment. In that study, factors such as construction material, load resistance system, height, and quality of construction were considered in building classification. Motamed et al. [40] developed fragility curves for 23 building classes based on construction material, building height, lateral load resisting system, and year of construction for residential buildings in Iran. Fallah Tafti et al. [41] developed fragility curves for 19 building classes in Iran by compiling a set of existing fragility curves and merging them based on the Analytic Hierarchy Approach (AHP). They also validated their model based on records of some past earthquakes in Iran. Bastami et al. [42] provided a set of 26 vulnerability curves for residential buildings in Iran by considering construction material, age, and building height. In the present study, the fragility curves proposed by Fallah Tafti et al. [41] are used due to the compatibility of the building classes in the present study. These fragility curves provide the probability of damages in four levels, including slight, moderate, extensive, and collapse.

5. Estimating seismic loss based on Mosha fault seismic scenario

This section provides probable seismic losses in the case of the Mosha fault seismic scenario in terms of residential building damages and the number of fatalities. To provide a realistic estimation of damages in a distributed exposure model, spatial correlation due to coherent contributions from source, path, and site should be

considered [43]. The impact of this factor on seismic loss assessment has been assessed in several studies. For example, Weatherill et al. [44] showed that disregarding spatial correlation in seismic risk assessment may underestimate the loss, especially in long return periods. In the present study, to consider spatial correlation in the analysis, random sampling from variability of ground motion values was performed, as shown in **Figure 4**. In general, variability from ground values can be categorized into two groups: inter-event variability and intra-event variability. The former represents variability from one earthquake to another, while the latter shows variability from one location to another [45,46]. While the variability of inter-event is sampled once for each synthetic event, intra-event uncertainty is sampled at each location. In the present study, we considered only one seismic scenario; thus, all variability in **Figure 4** can be considered as intra-event variability. Accordingly, the ground motion value at each location is determined based on Equation (6).

$$Ln\left(GMV_{ij}\right) = Ln(\overline{GMV}_{ij}) + \varepsilon_{ij}\sigma_{ij} \quad (6)$$

In the above equation, $\overline{GMV}_{ij}$ is the median ground motion value estimated by stochastic finite-fault model, σ_{ij} is intra-event variability, and ε is random coefficient from a spatial correlation model. Several spatial correlation models have been proposed by now [47,48]. Here, the model proposed by Zafarani et al. [49] is used. By compiling a reliable database of three components records from 461 Iran's earthquakes, they developed a spatial correlation for PGA and spectral acceleration. **Figure 9** shows the spatial correlation proposed by Zafarani et al. [49] in different spectral periods. As depicted, by increasing the separation distance, the spatial correlation is decreased; while the reduction in higher periods is lower than short periods.

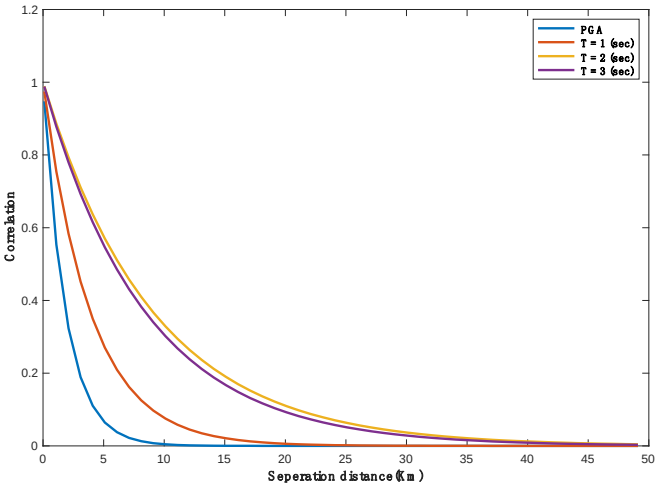

Figure 9. The spatial correlation proposed by Zafarani et al. [49] in different spectral periods.

The most important issue in the random sampling method is the number of iterations required to reach stable results. According to the law of large numbers, as the number of independent events increases, the distribution tends towards the normal distribution [50]. To this end, a sensitivity analysis was performed, and the results indicated that producing 100,000 iterations shows less than 5% variation in the median values of ground motion values. Thus, in the present study, the same number of

repetitions was performed. The distribution of mean damage ratio for Tehran (in a grid cell of 1 × 1 km) is shown in **Figure 10**. As depicted, the majority of damages occurred in the eastern and southern parts of Tehran, which experienced the highest acceleration. The high value of damages in the southern part of the city, which has a far distance from Mosha fault, is interesting. However, this could be mainly related to the concentration of many weak masonry structures in that region. The median of mean damage ratio from 100,000 iterations for the whole of Tehran is 6% ± 1.54%. This value is significantly lower than the estimated damage in the study of JICA [16], which assessed the damage ratio of Tehran for Mosha fault seismic scenario. This discrepancy can also be related to the years of studies and calculation methods. During recent years, many engineered structures have been constructed in Tehran based on the new seismic regulations. Thus, it is expected that the potential seismic loss in our study should be much lower than in the older one. In addition, JICA [16] used a deterministic approach based on the GMPEs for hazard estimation; however, in our study, the stochastic finite-fault method was employed for hazard evaluation.

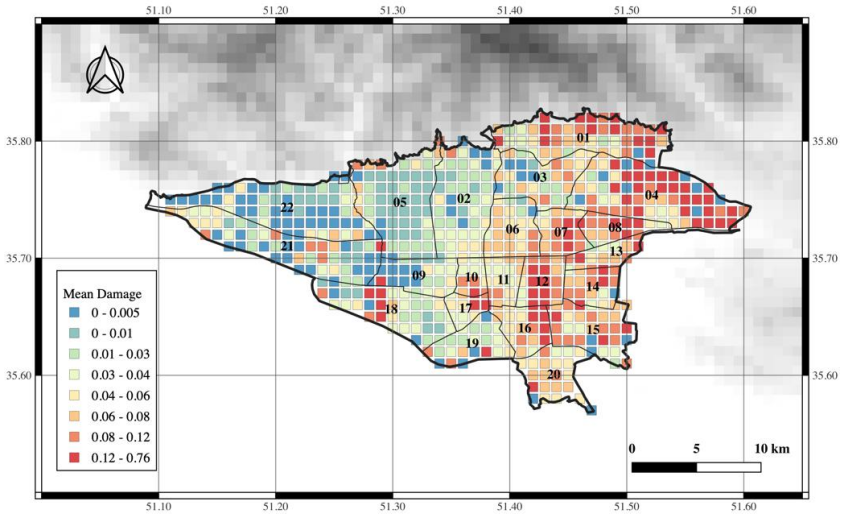

Figure 10. Distribution of mean damage ratio in Tehran.

Estimating the probable number of fatalities in the Mosha fault seismic scenario is another goal of this study. There are several approaches to estimate fatalities, which can be classified into two main groups: Non-damage-based and damage-based approaches. In the non-damage-based approach, earthquake fatalities are directly correlated with ground shaking intensity and population. However, this method is based on several assumptions and eliminates many explanatory variables [51–53]. In the damage-based approach, an estimation of damages in different classes of buildings is derived, and then, based on fatality rates of different building classes, the number of fatalities can be determined [35]. This approach allows for the effects of different types of buildings on fatality to be taken into account.

In the present study, the damage-based approach is employed. The main challenging issue regarding the damage-based approach is providing a reliable fatality rate in different building classes. At present, there is no global agreement on applicable fatality rates to be used in loss estimation models, and there is certainly a lack of comprehensive data collection in the field following actual events [54]. Thus, in the

present study, we used a judgment-based fatality rate for different building classes by considering information provided in peer-reviewed papers or guidelines (such as HAZUS). The fatality rate in different damage levels for the predefined building classes is presented in **Table 4**. As shown, it is assumed that there are no fatalities in the slight mode of damage in all building classes. In addition, due to a lack of data corresponding to different qualities of construction and heights of steel and concrete structures in past earthquakes, just one value of fatality rate was considered in this analysis. The highest fatality rate is also assigned to the masonry building classes. These buildings generally have no resistance to ground shaking and will completely collapse in strong earthquakes. Based on the aforementioned parameters, the total number of fatalities in the case of the Mosha fault seismic scenario for Tehran is estimated to be around 15,952. This is equivalent to 0.2 percent of the total population of the city. This is lower than the estimated value in the study of JICA [16], which proposed a value of 0.3 percent as the fatality ratio for Tehran. This is in accordance with our expectation because the damage ratio in the present study is lower than JICA [16]; consequently, it is expected that the fatality rate is also lower than JICA [16]. **Figure 11** shows the distribution of fatalities within grid cells. As depicted, again, the majority of victims are distributed in the eastern and central parts of the city, where they experience the highest damage (**Figure 10**).

Table 4. Fatality rate in different damage levels of pre-defined building classes.

Building classes	**Fatality rate in different damages level**			
	Slight	**Moderate**	**Extensive**	**Collapse**
ST-LR-LQ	-	-	5	15
ST-LR-MQ	-	-	5	15
ST-LR-HQ	-	-	5	15
ST-MR-LQ	-	-	5	15
ST-MR-MQ	-	-	5	15
ST-MR-HQ	-	-	5	15
ST-HR-LQ	-	-	5	15
ST-HR-MQ	-	-	5	15
ST-HR-HQ	-	-	5	15
RC-LR-LQ	-	-	5	15
RC-LR-MQ	-	-	5	15
RC-LR-HQ	-	-	5	15
RC-MR-LQ	-	-	5	15
RC-MR-MQ	-	-	5	15
RC-MR-HQ	-	-	5	15
RC-HR-LQ	-	-	5	15
RC-HR-MQ	-	-	5	15
RC-HR-HQ	-	-	5	15
MA-LR-LQ	-	5	10	35

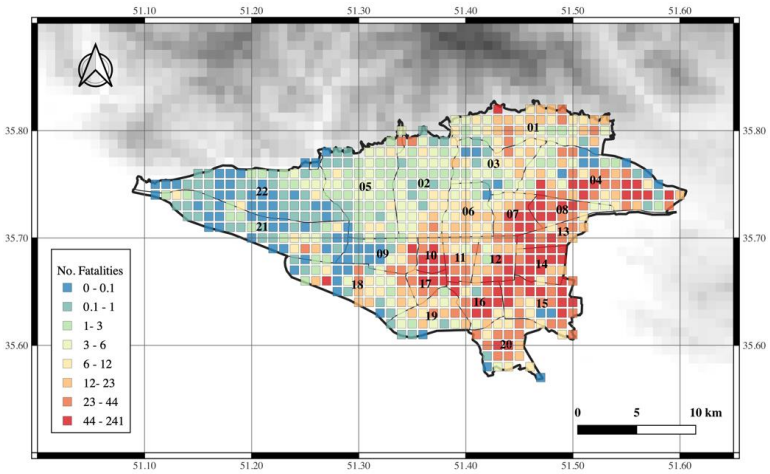

Figure 11. Distribution of fatalities in Tehran, in the case of Mosh seismic scenario.

It should be mentioned that due to contributing several factors in estimating the building damage and fatalities of an earthquake, the outcomes of this study are undoubtedly associated with uncertainties. However, these results can provide appropriate insight for emergency response authorities to develop appropriate action plans for the case of Mosha fault seismic scenario.

6. Conclusion

This paper presents an assessment of the probable seismic losses in Tehran, in terms of building damage and fatalities, that may result from a seismic event along the Mosha fault. To this end, the paper performs a comprehensive review of seismic risk components, which includes evaluating the seismic hazard, compiling an exposure model, and selecting appropriate fragility curves. The seismic hazard assessment employs the stochastic finite-fault method, an approach proposed by Motazedian [22], which is a robust tool considering source, path, and near-source effects. This method, treating earthquakes as a summation of point sources over a finite-fault plane, is well-suited for simulating time-history waveforms and estimating engineering parameters.

Given the absence of a recorded strong earthquake on the Mosha fault, model parameters such as stress drop, fault plane characteristics, and slip rate are inferred from geological, geotechnical, or data from similar historical earthquakes in Iran, like the Manjil-Roudbar earthquake in 1990. Although assumptions regarding model parameters introduce uncertainties into the results, this remains the only viable approach in the absence of real data from a significant seismic event in Tehran.

The study indicates that the Peak Ground Acceleration (PGA) in Tehran for a Mosha fault seismic scenario range from 0.05 g to 0.4 g. The highest accelerations are likely to be experienced in the eastern and central parts of the city, attributed to their proximity to the Mosha fault and the presence of soft soil in these areas. For validation, the simulated PGA values were compared with those from NGA-West2 Ground Motion Prediction Equations (GMPEs), showing reasonable agreement.

Building exposure models were compiled using data provided by the Statistical Center of Iran [3], which currently stands as the most comprehensive source of information on building characteristics in Iran. In this research, buildings are categorized into 19 groups based on construction material, age, and height. Moreover,

a set of fragility curves suggested by Fallah Tafti et al. [41] were employed to assess building damages. To account for intra-event variability in the analysis, a random sampling involving 100,000 iterations was conducted, each iteration generating a ground motion shaking map along with a randomly chosen value of intra-event uncertainty derived from a spatial correlation model. The median mean damage ratio derived from these iterations for Tehran is 6% ± 1.54%, with the highest damages predicted for the eastern and central parts of the city, which are also the areas most vulnerable to acceleration.

Fatality estimations were computed using a damage-based approach, wherein a judgment-based fatality rate was applied to different building classes to determine the likely number of victims from the Mosha fault seismic scenario. The estimations suggest that there could be 15,952 fatalities, which is approximately 0.2 percent of Tehran's total population. Furthermore, the distribution of fatalities across Tehran indicates that the most critical areas are the central and eastern parts, where many low-income residents live. It is imperative for local authorities to develop effective seismic risk mitigation strategies for these areas.

It is important to note that the study's conclusions, including both fatality and damage estimates, involve several explanatory parameters, which means they are subject to some degree of uncertainty. Despite this, the findings offer significant insights that can aid local disaster management authorities in devising necessary emergency response and preparedness plans.

Author contributions: Material preparation, data collection and analysis, NK and EF; the seismic hazard analysis, RA; the figures and material, OM; preparing the codes, AA; the first draft of the manuscript, EF; commented on manuscript, NK. All authors have read and agreed to the published version of the manuscript.

Acknowledgments: This paper presents some parts of the results of a project carried out in International Institute of Earthquake Engineering and Seismology (IIEES), Tehran. The financial and technical supports of this institute are highly appreciated. The authors also gratefully appreciate all individuals and organizations contributing to the compiling data sets used in the present study, particularly the Statistical Center of Iran (SCI) for providing the building inventories and population database.

Conflict of interest: The authors declare no conflict of interest.

References

1. Tchalenko JS, Braud J, Berberian M. Discovery of three earthquake faults in Iran. Nature. 1974, 248(5450): 661-663. doi: 10.1038/248661a0
2. Jackson J, McKenzie D. Active tectonics of the Alpine--Himalayan Belt between western Turkey and Pakistan. Geophysical Journal International. 1984, 77(1): 185-264. doi: 10.1111/j.1365-246x.1984.tb01931.x
3. Statistical Centre of Iran (SCI), Statistical Centre of Iran, Vice-Presidency for Strategic Planning and Supervision. National Census of Population and Housing Techical Reports, Sarshomāri 2016 (1395), 2011 (1390), 2006 (1385), 1996 (1375), 1986 (1365), and 1976 (1355): Tehran. formerly, the Plan & Budget Organization of the Imperial Government of Iran, Statistical Centre; 2016.
4. Berberian M. Contribution to the Seismotectonics of Iran II. 1976.
5. Moinfar A, Mahdavian A, Maleki E. Historical and instrumental earthquake data collection of Iran. Publication Iranian Culture. Affairs Inst, Tehran; 1994. p. 446.

6. Jalalalhosseini SM, Zafarani H, Zare M. Time-dependent seismic hazard analysis for the Greater Tehran and surrounding areas. Journal of Seismology. 2017, 22(1): 187-215. doi: 10.1007/s10950-017-9699-4
7. Berberian M, Yeats RS. Tehran: An earthquake time bomb. 2017.
8. Firuzi E, Ansari A, Amini Hosseini K, et al. Probabilistic earthquake loss model for residential buildings in Tehran, Iran to quantify annualized earthquake loss. Bulletin of Earthquake Engineering. 2019, 17(5): 2383-2406. doi: 10.1007/s10518-019-00561-z
9. Kalantari M, Firuzi E, Ahmadipour masoud, et al. Estimating Annualized Earthquake Loss for Residential Buildings in Tehran, Iran. 2022. doi: 10.21203/rs.3.rs-1685779/v1
10. Firuzi E, Ansari A, Amini Hosseini K, Kheirkhah N. Developing an earthquake damaged-based multi-severity casualty method by using Monte Carlo simulation and fuzzy logic; case study: Mosha fault seismic scenario, Tehran, Iran. Stochastic Environmental Research and Risk Assessment. 2024, 1-21.
11. De Martini PM, Hessami K, Pantosti D, et al. A geologic contribution to the evaluation of the seismic potential of the Kahrizak fault (Tehran, Iran). Tectonophysics. 1998, 287(1-4): 187-199. doi: 10.1016/s0040-1951(98)80068-1
12. Nazari H, Ritz JF, Salamati R, et al. Morphological and palaeoseismological analysis along the Taleghan fault (Central Alborz, Iran). Geophysical Journal International. 2009, 178(2): 1028-1041. doi: 10.1111/j.1365-246x.2009.04173.x
13. Ritz JF, Nazari H, Balescu S, et al. Paleoearthquakes of the past 30,000 years along the North Tehran Fault (Iran). Journal of Geophysical Research: Solid Earth. 2012, 117(B6). doi: 10.1029/2012jb009147
14. Ambraseys NN, Melville CP. A history of Persian earthquakes. Cambridge University Press; 1982. p. 219.
15. Berberian M, Yeats RS. Patterns of historical earthquake rupture in the Iranian Plateau. Bulletin of the Seismological Society of America. 1999, 89(1): 120-139. doi: 10.1785/bssa0890010120
16. Japan International Cooperation Agency (JICA). The Study on Seismic Microzoning of the Greater Tehran Area in the Islamic Republic of Iran, Final Report, Japan International Cooperation Agency (JICA), Centre for Earthquake and Environmental Studies of Tehran (CEST) Tehran Municipality; 2000.
17. Beresnev IA. Source Parameters of Earthquakes in Eastern and Western North America Based on Finite-Fault Modeling. Bulletin of the Seismological Society of America. 2002, 92(2): 695-710. doi: 10.1785/0120010101
18. Zafarani H, Noorzad A, Ansari A, et al. Stochastic modeling of Iranian earthquakes and estimation of ground motion for future earthquakes in Greater Tehran. Soil Dynamics and Earthquake Engineering. 2009, 29(4): 722-741. doi: 10.1016/j.soildyn.2008.08.002
19. Saffari H, Roohafzayan A, Mahdavian A, Yari M. Stochastic Finite Fault Modeling and Simulation of Strong Ground Motion of Mosha Fault in Iran. Electronic Journal of Structural Engineering. 2020, 20: 63-71. doi: 10.56748/ejse.20247
20. Yu R, Song Y, Guo X, et al. Seismic hazard analysis for engineering sites based on the stochastic finite-fault method. Earthquake Science. 2022, 35(5): 314-328. doi: 10.1016/j.eqs.2022.05.007
21. Douglas J, Aochi H. A Survey of Techniques for Predicting Earthquake Ground Motions for Engineering Purposes. Surveys in Geophysics. 2008, 29(3): 187-220. doi: 10.1007/s10712-008-9046-y
22. Motazedian D. Stochastic Finite-Fault Modeling Based on a Dynamic Corner Frequency. Bulletin of the Seismological Society of America. 2005, 95(3): 995-1010. doi: 10.1785/0120030207
23. Boore DM. Stochastic simulation of high-frequency ground motions based on seismological models of the radiated spectra. Bull Seismol Soc Am. 1983, 73: 1865-1894.
24. Boore DM. Simulation of Ground Motion Using the Stochastic Method. Pure and Applied Geophysics. 2003, 160(3): 635-676. doi: 10.1007/pl00012553
25. Aki K. Scaling law of seismic spectrum. Journal of Geophysical Research. 1967, 72(4): 1217-1231. doi: 10.1029/jz072i004p01217
26. Landgraf A, Ballato P, Strecker MR, et al. Fault-kinematic and geomorphic observations along the North Tehran Thrust and Mosha Fasham Fault, Alborz mountains Iran: implications for fault-system evolution and interaction in a changing tectonic regime. Geophysical Journal International. 2009, 177(2): 676-690. doi: 10.1111/j.1365-246x.2009.04089.x
27. Tatar M, Hatzfeld D, Abbassi A, et al. Microseismicity and seismotectonics around the Mosha fault (Central Alborz, Iran). Tectonophysics. 2012, 544-545: 50-59. doi: 10.1016/j.tecto.2012.03.033
28. Solaymani Azad S, Ritz JF, Abbassi MR. Left-lateral active deformation along the Mosha–North Tehran fault system (Iran): Morphotectonics and paleoseismological investigations. Tectonophysics. 2011, 497(1-4): 1-14. doi: 10.1016/j.tecto.2010.09.013

29. Wells DL, Coppersmith KJ. New empirical relationships among magnitude, rupture length, rupture width, rupture area, and surface displacement. Bulletin of the Seismological Society of America. 1994, 84(4): 974-1002. doi: 10.1785/bssa0840040974
30. Motazedian D. Region-Specific Key Seismic Parameters for Earthquakes in Northern Iran. Bulletin of the Seismological Society of America. 2006, 96(4A): 1383-1395. doi: 10.1785/0120050162
31. Heaton TH. Evidence for and implications of self-healing pulses of slip in earthquake rupture. Physics of the Earth and Planetary Interiors. 1990, 64(1): 1-20. doi: 10.1016/0031-9201(90)90002-f
32. ATC (Applied Technology Council). Earthquake damage evaluation data for California, ATC-13. Redwood City, CA; 1985.
33. Grunthal G. European macroseismic scale 1998 (EMS-98). Cahiers du Centre Europeen de Geodynamique et de Seismologie 15, Centre Europeen de Geodynamique et de Seismologie, Luxembourg; 1998.
34. FEMA (Federal Emergency Management Agency). HAZUS- MH MR4 technical manual. Washington, DC: FEMA; 2003.
35. Jaiswal K, Wald DJ. Creating a Global Building Inventory for Earthquake Loss Assessment and Risk Management. Open-File Report; 2008. doi: 10.3133/ofr20081160
36. Crowley H, Colombi M, Silva V, et al. D3.1 Fragility functions for common RC building types in Europe. 2011.
37. Silva V, Brzev S, Scawthorn C, et al. A Building Classification System for Multi-hazard Risk Assessment. International Journal of Disaster Risk Science. 2022, 13(2): 161-177. doi: 10.1007/s13753-022-00400-x
38. Omidvar B, Gatmiri B, Derakhshan S. Experimental vulnerability curves for the residential buildings of Iran. Natural Hazards. 2011, 60(2): 345-365. doi: 10.1007/s11069-011-0019-y
39. Sadeghi M, Ghafory-Ashtiany M, Pakdel-Lahiji N. Developing seismic vulnerability curves for typical Iranian buildings. Proceedings of the Institution of Mechanical Engineers, Part O: Journal of Risk and Reliability. 2015, 229(6): 627-640. doi: 10.1177/1748006x15596085
40. Motamed H, Calderon A, Silva V, et al. Development of a probabilistic earthquake loss model for Iran. Bulletin of Earthquake Engineering. 2018, 17(4): 1795-1823. doi: 10.1007/s10518-018-0515-5
41. Fallah Tafti M, Amini Hosseini K, Mansouri B. Generation of new fragility curves for common types of buildings in Iran. Bulletin of Earthquake Engineering. 2020, 18: 3079-3099.
42. Bastami M, Abbasnejadfard M, Motamed H, et al. Development of hybrid earthquake vulnerability functions for typical residential buildings in Iran. International Journal of Disaster Risk Reduction. 2022, 77: 103087. doi: 10.1016/j.ijdrr.2022.103087
43. Verros SA, Wald DJ, Worden CB, et al. Computing spatial correlation of ground motion intensities for ShakeMap. Computers & Geosciences. 2017, 99: 145-154. doi: 10.1016/j.cageo.2016.11.004
44. Weatherill GA, Silva V, Crowley H, Bazzurro P. Exploring the impact of spatial correlations and uncertainties for portfolio analysis in probabilistic seismic loss estimation. Bulletin of Earthquake Engineering. 2015, 13: 957-981.
45. Silva V. Critical Issues on Probabilistic Earthquake Loss Assessment. Journal of Earthquake Engineering. 2017, 22(9): 1683-1709. doi: 10.1080/13632469.2017.1297264
46. Crowley H, Bommer JJ. Modelling Seismic Hazard in Earthquake Loss Models with Spatially Distributed Exposure. Bulletin of Earthquake Engineering. 2006, 4(3): 249-273. doi: 10.1007/s10518-006-9009-y
47. Goda K, Atkinson GM. Probabilistic Characterization of Spatially Correlated Response Spectra for Earthquakes in Japan. Bulletin of the Seismological Society of America. 2009, 99(5): 3003-3020. doi: 10.1785/0120090007
48. Jayaram N, Baker JW. Correlation model for spatially distributed ground-motion intensities. Earthquake Engineering & Structural Dynamics. 2009, 38(15): 1687-1708. doi: 10.1002/eqe.922
49. Zafarani H, Ghafoori SMM, Adlaparvar MR. Spatial Correlation of Peak Ground Motions and Pseudo Spectral Acceleration Based on the Iranian Multievent Datasets. Journal of Earthquake Engineering. 2021, 26(12): 6042-6062. doi: 10.1080/13632469.2021.1911882
50. Rohatgi VK, Saleh AKMdE. An Introduction to Probability and Statistics. Wiley Series in Probability and Statistics. John Wiley and Sons; 2015. doi: 10.1002/9781118799635
51. Badal J, Vazquez-prada M, Gonzalez A. Preliminary Quantitative Assessment of Earthquake Casualties and Damages. Natural Hazards. 2005, 34(3): 353-374. doi: 10.1007/s11069-004-3656-6
52. Firuzi E, Amini Hosseini K, Ansari A, et al. An empirical model for fatality estimation of earthquakes in Iran. Natural Hazards. 2020, 103(1): 231-250. doi: 10.1007/s11069-020-03985-y

53. Firuzi E, Amini Hosseini K, Ansari A, et al. Developing a new fatality model for Iran's earthquakes using fuzzy regression analysis. International Journal of Disaster Risk Reduction. 2022, 80: 103231. doi: 10.1016/j.ijdrr.2022.103231
54. So E. Estimating Fatality Rates for Earthquake Loss Models. Springer International Publishing; 2016. doi: 10.1007/978-3-319-26838-5